Title

Enhanced Stability and Efficiency for Photoelectrochemical Iodide Oxidation by Methyl Termination and Electrochemical Pt Deposition on n-Type Si Microwire Arrays

Permalink

https://escholarship.org/uc/item/7r75g2bx

Journal

ACS Energy Letters, 4(9)

ISSN

2380-8195

Authors

Ardo, Shane
Santori, Elizabeth A
Emmer, Hal S
et al.

Publication Date

2019-09-13

DOI

10.1021/acsenergylett.9b01529

Supplemental Material

https://escholarship.org/uc/item/7r75g2bx#supplemental

ACS Energy LETTERS

Cite This: ACS Energy Lett. 2019, 4, 2308−2314

http://pubs.acs.org/journal/aelccp

Enhanced Stability and Efficiency for Photoelectrochemical Iodide Oxidation by Methyl Termination and Electrochemical Pt Deposition on n-Type Si Microwire Arrays

Shane Ardo,[†] Elizabeth A. Santori,[†] Hal S. Emmer,[‡] Ronald L. Grimm,[†] Matthew J. Bierman,[†] Bruce S. Brunschwig,[§] Harry A. Atwater,[‡,∥] and Nathan S. Lewis*[,†,§,∥]

[†]Division of Chemistry and Chemical Engineering, California Institute of Technology, 1200 East California Blvd., Pasadena, California 91125, United States

[‡]Thomas J. Watson Laboratories of Applied Physics, California Institute of Technology, 1200 East California Blvd., Pasadena, California 91125, United States

[§]Beckman Institute, California Institute of Technology, 1200 East California Blvd., Pasadena, California 91125, United States

[∥]Kavli Nanoscience Institute, California Institute of Technology, 1200 East California Blvd., Pasadena, California 91125, United States

Supporting Information

ABSTRACT: **Arrays of Si microwires doped n-type (n-Si) and surface-functionalized with methyl groups have been used, with or without deposition of Pt electrocatalysts, to photoelectrochemically oxidize I^-(aq) to I_3^-(aq) in 7.6 M HI(aq). Under conditions of iodide oxidation, methyl-terminated n-Si microwire arrays exhibited stable short-circuit photocurrents over a time scale of days, albeit with low energy-conversion efficiencies. In contrast, electrochemical deposition of Pt onto methyl-terminated n-Si microwire arrays consistently yielded energy-conversion efficiencies of ∼2% for iodide oxidation, with an open-circuit photovoltage of ∼400 mV and a short-circuit photocurrent density of ∼10 mA cm^{-2} under 100 mW cm^{-2} of simulated air mass 1.5G solar illumination. Platinized electrodes were stable for >200 h of continuous operation, with no discernible loss of Si or Pt. Pt deposited using electron-beam evaporation also resulted in stable photoanodic operation of the methyl-terminated n-Si microwire arrays but yielded substantially lower photovoltages than when Pt was deposited electrochemically.**

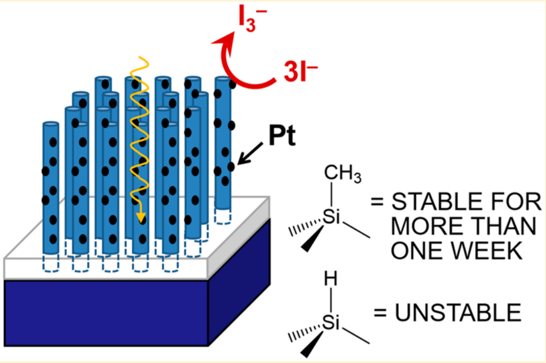

Global climate change caused by anthropogenic greenhouse gases is a serious concern. To help mitigate this, solar energy utilization is particularly attractive because solar panels are easily deployable on various size scales. Further, in many regions of the world electricity from solar panels is cost-competitive with electricity derived from sources that emit greenhouse gases.[1,2] However, at certain times of the day solar panels may provide more electricity than demanded. This situation can occur at a level of solar panel installation that provides as little as ∼20% of the daily electricity demand,[3,4] therefore necessitating substantial installment of energy storage technologies to enable 100% renewable electricity generation to be effectively utilized. Silicon represents over 90% of the installed solar panel capacity,[1] and hence, identification of uses for silicon for direct light-to-chemical energy storage is of current technological interest. Arrays of Si microwires (MWs)[5−14] and nanowires[15−23] are interesting platforms for the fabrication of artificial photosynthetic devices. The high aspect ratio of the wires allows for effective light absorption along the length of the wire, while enabling short, radial charge-carrier collection distances to electrocatalysts optimally integrated in a high-surface-area structure.[24] The porosity of the wire array allows for facile reactant access and product egress to/from the internal area of the morphologically structured light absorber and provides a minimal path length for ionic conduction to and through a supporting membrane.[25]

Received: July 17, 2019
Accepted: July 24, 2019
Published: July 25, 2019

DOI: 10.1021/acsenergylett.9b01529
ACS Energy Lett. 2019, 4, 2308−2314

Renewable energy storage using H_2 from water or fuels from direct CO_2 reduction from the atmosphere represent particularly interesting chemical storage options because they form simple high-energy-density chemicals and/or are carbon neutral processes. However, both of these reactions present major challenges,[26] because both reactions utilize electrons and protons from water via its oxidation to O_2 by a complex four-electron, four-proton process to store >1.0 V of potential. This kinetically challenging process has only ∼40% roundtrip efficiency for H_2 energy storage via water electrolysis and use in a polymer−electrolyte−membrane fuel cell.[27,28] Moreover, the band gap of Si is 1.12 eV, and even state-of-the-art Si photovoltaics typically exhibit photovoltages at their maximum power point of only ∼0.6 V under 1 Sun illumination.[29] Hence, Si by itself, either as an individual light absorber or in a tandem structure in which two Si light absorbers are arranged optically and electrically in series, cannot provide the photovoltage necessary to drive water electrolysis or sustainable CO_2 reduction.[30] Si is also unstable toward anodic oxidation in aqueous electrolytes and thus benefits from kinetic stabilization strategies such as use of one-electron-transfer redox species in nonaqueous solvents or protective coatings.[31−34]

Identification of simple alternative electron sources to water are timely research endeavors. Halides in particular allow for ∼90% roundtrip efficiency for H_2 energy storage and use.[28,35] Therefore, photoelectrolysis of HI(aq) to produce H_2(g) and I_3^-(aq) is one potential approach for solar energy storage using a Si light absorber. The minimum voltage needed for the electrolysis reaction is ∼0.55 V under standard-state conditions[36] and is only ∼0.25 V in highly concentrated HI(aq),[37] both of which can be provided by single, nontandem Si MW arrays.[38−40] A demonstration of the utility of Si MW arrays for the unassisted electrolysis of HI(aq) would also provide a pathway toward technologies for solar fuel production. Such a demonstration, however, requires a method to suppress the anodic oxidation/passivation of Si in aqueous solutions. Unassisted photoelectrolysis of HI(aq) has been demonstrated using membrane-embedded p-type Si MW arrays in which the Si MWs served as the photocathode and iodide was oxidized at a back metal contact to the MWs.[41] Moreover, planar single-crystalline n-Si(111) photoanodes have been shown to be stable in contact with Fe-$(CN)_6^{3-/4-}$(aq) solutions for hours of continuous illumination, if the Si surface is terminated with methyl groups.[42] Methyl termination also introduces a surface dipole that shifts the band edges relative to the solution redox potential, which increases the photovoltage relative to that of H-terminated n-Si(111) photoelectrodes.[43] We demonstrate herein the use of methyl-terminated Si MWs, in conjunction with surface-bound Pt electrocatalysts for I^- oxidation, to enhance the stability of n-Si MW array electrodes under photoanodic operation while effecting the solar-driven oxidation of I^-(aq) to I_3^-(aq) in 7.6 M HI(aq) at an ideal regenerative-cell energy-conversion efficiency,[41] η_{IRC}, of >1% for >200 h of continuous operation under 1 Sun of simulated air mass (AM) 1.5 G solar illumination (Figure 1).

Crystalline Si MW arrays were grown by the vapor−liquid−solid growth method on patterned (111)-oriented Si substrates.[41,44,45] The desired MW diameter and spacing were produced by lithographically patterning 3 μm diameter circular holes, with a center-to-center pitch of 7 μm, into an oxide overlayer on a degenerately doped, nonphotoactive Si(111) substrate.[45] The holes in the oxide layer were subsequently filled with thermally evaporated Cu, which served as the Si growth catalyst. The doping type and dopant density of the n-Si MWs was controlled by use of PH_3 during growth, with the height of the MWs controlled by the growth time and the position of the substrate in the reactor. After growth and cleaning, the n-Si MW arrays were functionalized with methyl groups by a two-step chlorination−alkylation reaction sequence.[43,46−48] As needed, Pt was then deposited using electron-beam evaporation or by electrochemical deposition from 5 mM K_2PtCl_4(aq) by passing >100 mC cm^{-2} of cathodic charge density at −1.0 V versus a saturated calomel electrode (SCE) (additional details are available in the Supporting Information).

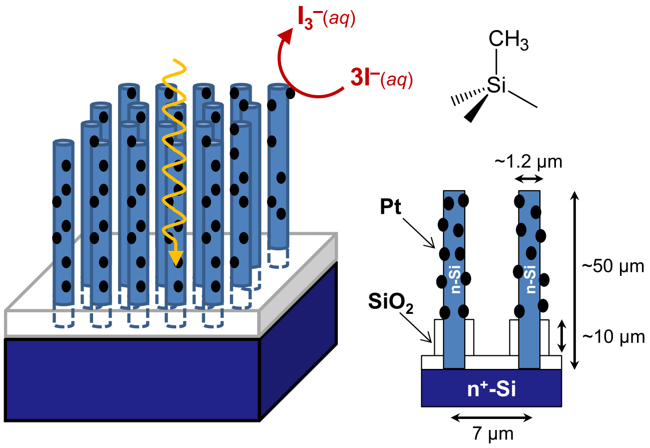

Figure 1. Si MW array photoanode that is the focus of this work and effects the stable light-driven oxidation of I^-(aq) to I_3^-(aq) in 7.6 M HI(aq). The MWs are doped n-type, are surface-terminated with methyl groups, contain surface-bound Pt electrocatalysts, and contain an oxide boot to attenuate electrochemical shunts.

Four-point probe measurements on single Si MWs yielded calculated resistivities, and therefore calculated dopant densities,[15] that were not related linearly to the partial pressure of the PH_3 dopant gas used during MW growth (Figure S1). Measurements on the n-Si MWs that were etched by KOH(aq) suggested that the MW shells were more conductive than the cores. The radial dependence of the dopant density is consistent with deposition of excess P by a vapor−solid−solid growth mechanism.[49,50] A high-temperature thermal oxide "booting" procedure was then applied to distribute the dopants more homogeneously throughout the radius of the MW and to etch some of the excess dopants from the MW shell prior to thermal annealing. This booting process was required to obtain high-quality MW arrays that exhibited current density versus potential (*J*−*E*) behavior (Figure S2) consistent with that previously reported in nonaqueous electrolytes containing a one-electron, outer-sphere ferrocene-based redox couple.[45] The normal-incidence spectral response under these conditions (Figure S3) was similar to that reported previously for p-type or intrinsic (i.e., unintentionally doped) Si MW arrays[51,52] but was n-type in character for these n-Si MW arrays. Changing the orientation of the Si MW arrays with respect to the direction of propagation of incoming light has been shown to result in increased external quantum yields, even beyond the limit imposed by ergodic ray-optic light trapping.[51] In addition, improved light management techniques using, for example, arrays of microcones can yield high absorption over a large range of angles of the incident illumination.[53] Consistently, in the dark the MW arrays exhibited current rectification, evidenced by passing substantial cathodic currents at negative potentials in conjunction with small anodic currents at positive potentials (Figures S2 and S4).

Figure 2 displays representative photoelectrochemical J−E data of *planar*, single-crystalline n-Si(111) electrodes in contact with Ar-purged ~7.6 M HI(aq) that by visual inspection contained adventitious I_3^-(aq). The surfaces were as follows: H−Si(111) (blue); Pt deposited electrochemically on H−Si(111) (purple); CH_3−terminated Si(111) (brown); Pt deposited electrochemically on CH_3−terminated Si(111) (green); or Pt deposited using electron-beam evaporation on CH_3-terminated Si(111) (red). Even in highly concentrated ~7.6 M I^-(aq), the H-terminated n-Si(111) electrodes exhibited a large resistance near open-circuit conditions, low fill factors, and a rapid degradation of performance under illumination. This loss in performance is attributed to oxidation/passivation of the Si surface under photoanodic operation. Deposition of Pt without prior methylation provided enhanced rates of I^- oxidation but low stability, similar to that observed for H-terminated Si(111). CH_3 termination alone resulted in an electrode that was stable on the time scale of days but exhibited a very low fill factor, attributable to the slow interfacial charge-transfer rate constant for the oxidation of I^- at Si surfaces.[54,55] Open-circuit voltages, V_{oc}, for CH_3-terminated n-Si(111) photoelectrodes were consistently larger than those observed for H-terminated n-Si(111) photoelectrodes, regardless of whether electrochemically deposited Pt was present. This behavior is consistent with expectations in which an interfacial surface dipole arising from Si−CH_3 bonds produces a negative shift in the band-edge positions of CH_3−Si(111) surfaces relative to H−Si(111) surfaces.[43,56,57] In contrast to the other electrodes, CH_3 termination in combination with electrochemical deposition of Pt produced large fill factors and resulted in planar n-Si photoanodes that exhibited reproducible, stable, and efficient photooxidation of HI(aq).[37] Hence, through judicious choice of the Pt deposition protocol, large photovoltages could be obtained even though Pt typically forms interfacial silicides that limit the photovoltage to <500 mV under 1 Sun illumination,[58] similar to the behavior we observed for Pt deposited by electron-beam evaporation.

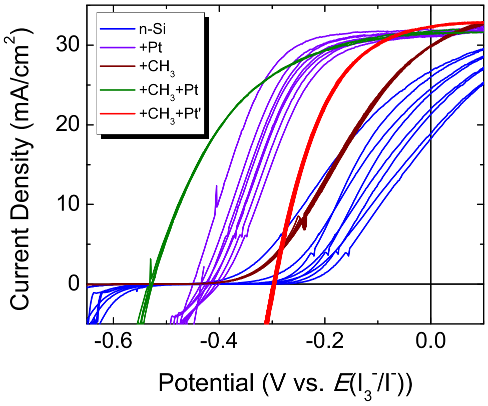

Figure 2. Three-electrode current density versus potential data recorded under 100 mW cm^{-2} of simulated AM1.5G solar illumination for *planar*, single-crystalline, n-type Si(111) electrodes immersed in Ar-purged ~7.6 M HI(aq) containing adventitious I_3^- with or without (blue) various combinations of surface terminations and catalyst treatments: methylation (+CH_3), electrochemical Pt deposition (+Pt), and electron-beam evaporation of Pt (+Pt′).

Figure 3 displays representative photoelectrochemical J−E performance of a methylated n-Si MW array electrode in contact with ~7.6 M HI(aq), before and after electrochemical deposition of Pt. Methylated n-Si MW arrays were not easily wetted by water or aqueous electrolytes. Repeated immersion of electrodes into either of these solutions (~10 times) resulted in electrochemical contact between the aqueous electrolyte and the MW arrays suitable for measurements. Methylated n-Si MW arrays that contained electrochemically deposited Pt consistently exhibited $V_{oc} \approx 400$ mV; short-circuit current densities, J_{sc}, of ~10 mA cm^{-2} at the Nernstian potential for oxidation of I^- to I_3^-, $E(I_3^-/I^-)$; and an ideal regenerative-cell energy-conversion efficiency, η_{IRC}, of ~2.0% under 1 Sun of simulated AM1.5G solar illumination. Figure S4 shows the behavior of the best-performing sample measured during the course of this work.

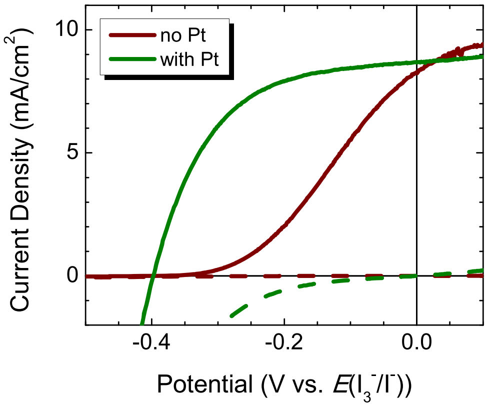

Figure 3. Three-electrode current density versus potential data recorded in the dark (dashed) or under 100 mW cm^{-2} of simulated AM1.5G solar illumination (solid lines) for a methylated n-type Si MW array electrode immersed in Ar-purged ~7.6 M HI(aq) electrolyte containing adventitious I_3^- before (brown) or after (green) electrochemical deposition of Pt.

Prior studies reported that methyl-termination of *planar*, single-crystalline n-Si(111) surfaces followed by Pt deposition resulted in efficient and stable photocurrent for the photooxidation of aqueous iodide or bromide.[17,37,59] Photocurrents for I^- oxidation using H-terminated n-Si *nanowires* with surface-deposited Pt and without surface methylation were shown to exhibit modest stability on the time scale of days.[37] However, the platinized n-Si MW arrays without methyl groups investigated herein consistently exhibited poor stability for I^-(aq) oxidation. In contrast, the n-Si MW arrays that had been platinized after methyl-termination showed stable photocurrents for >200 h of near-continuous I^-(aq) photooxidation, with J_{sc} decreasing by <15% after 200 h of continuous cyclic voltammetric sweeping (Figure 4). This decrease in J_{sc} over time is consistent with our observation of light attenuation by photogenerated I_3^- measured using a calibrated silicon photodiode. However, the change in the shape of the J−E behavior to one that is consistent with increased shunting suggests that oxidation of the surface of the MWs was likely. This is not surprising given expected imperfect methylation of the non-Si(111) facets on the

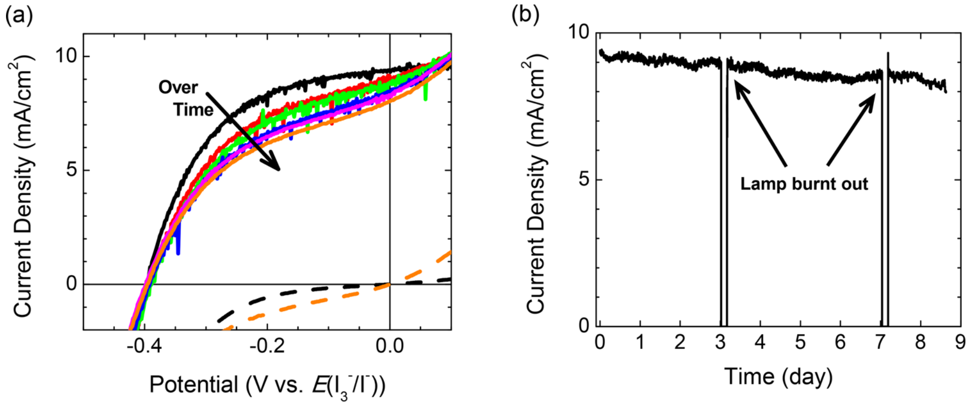

Figure 4. (a) Three-electrode current density versus potential data recorded in the dark (dashed; black initially and orange after 200 h) or under 100 mW cm^{-2} of simulated AM1.5G solar illumination every 50 h, and at 200 h of near-continuous illumination, for the methylated n-type Si MW array electrode with electrochemically deposited Pt of Figure 3 immersed in Ar-purged ~7.6 M HI(aq) containing adventitious I_3^-. (b) Three-electrode chronoamperometry data recorded at a potentiostatic bias of 0 V versus the Nernstian potential of the solution over 200 h of 100 mW cm^{-2} of simulated AM1.5G solar illumination, which totalled 207.5 h to compensate for the instances when the ELH-type W-halogen lamp burnt out and was replaced with a new source.

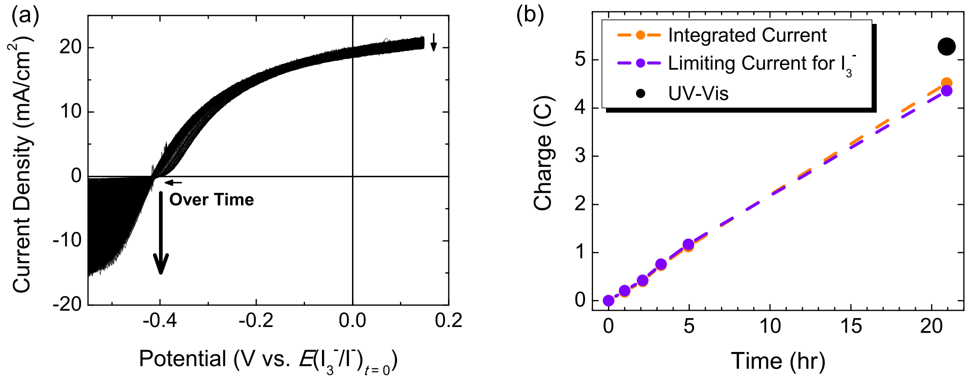

Figure 5. (a) Three-electrode current density versus potential data in an H-cell configuration with the working and counter electrodes separated by a Nafion membrane recorded continuously at a scan rate of 10 mV s^{-1} under 100 mW cm^{-2} of simulated AM1.5G solar illumination for a methylated n-type Si MW array electrode with electrochemically deposited Pt immersed in Ar-purged ~7.6 M HI(aq) that initially contained adventitious I_3^- over ~21 h of continuous operation. (b) Integrated current data from panel a reported for several times during the measurement (orange) and the scaled limiting cathodic current near −0.55 V, which is proportional to the amount of I_3^- in solution. For reference, also shown is the end point concentration of I_3^- determined using ultraviolet−visible (UV−Vis) electronic absorption spectroscopy in conjunction with the Beer−Lambert law.

sidewalls of the MWs due to varied bonding environments and sterics.[60] A methyl-terminated n-Si MW array that did not contain Pt exhibited stable, but modest, efficiency under the same conditions (Figure S5). This observation is consistent with expectations of stable but attenuated performance for methyl-terminated *planar*, single-crystalline n-Si(111) electrodes in the absence of Pt catalysts (Figure 2).

To assess the feasibility of performing the overall photoelectrolysis of aqueous hydriodic acid, in which the concentration of I_3^- will increase substantially over time, as well as to assess the quantum yield of I_3^- formation, *J*−*E* data under potentiostatic control were obtained over 21 h for a platinized, methyl-terminated n-Si MW array in ~7.6 M HI(aq) that initially contained adventitious I_3^-. These data were obtained in a three-electrode setup in an H-cell configuration in which the working electrode was separated from the Pt counter electrode by a Nafion membrane (Figure 5a). Ex situ spectroscopic detection indicated near unity Faradaic yield for formation of I_3^-(aq) (Figure 5b). Consistently, the total anodic charge passed directly correlated with the cathodic limiting current densities ascribable to reduction of I_3^- at the Si MW array photoelectrode. The number of turnovers per Si atom was ~900 (see the Supporting Information for calculation), implying that >200-fold excess of charge was passed relative to the amount of charge required to fully oxidize each Si atom via a four-hole process. No discernible loss of Si was observed via scanning-electron microscopy before and after the evaluation period of 21 h (Figure S6), supporting that Si etching and/or loss of Pt was not responsible for the small decrease in photoanodic current density as a function of operating time. After the electrolysis, a calibrated Si photodiode that was placed in the cell close to the position of the MW array exhibited ~85% of its initial response before the electrolysis, consistent with the observed decrease in photocurrent from the Si MW photoanode and indicating that the decay can be ascribed to parasitic light absorption due to the formation of I_3^- in the cell during the electrolysis. Moreover, the photoactivity was due to the MWs and not the substrate, because physical removal of the MWs yielded planar n-Si electrodes that exhibited little anodic photocurrent under the same conditions, as expected for degenerately doped n-Si(111) acting as the electrode.

Methylation, and in general surface functionalization via solution chemistry, is one of several approaches to protect underlying semiconductors from deleterious surface reactions.[61] Other protection schemes include physical deposition of materials, for example, by atomic-layer deposition (ALD), sputtering, evaporation, bombardment with atoms or molecules (e.g., nitridation[62]), or use of single-layer coatings including graphene.[63] Introduction of surface functionality using solution chemistry can provide a conformal coating, for which electron transfer across the interface is either mediated by this layer or requires tunnelling through insulating molecules,[64−66] such as for the methyl functionality utilized herein. However, even thin conformal layers of metals and metal-oxide materials can absorb and/or reflect a substantial amount of incoming light.[67] Moreover, coating high-surface-area substrates such as MW arrays and mesoporous thin films is challenging. Use of both surface chemistry and metal electrocatalysts resulted herein in a large V_{oc} due to the Si−CH_3 surface dipole as well as rapid catalysis from the Pt, resulting simultaneously in a large fill factor for iodide oxidation. Methylation additionally protected the Si surface from extensive oxidation.

The standard electrochemical potential required to oxidize I^-(aq) to I_3^-(aq) at unity activity for each species ($E^o(I_3^-/I^-)$) is ∼+0.55 V versus the normal hydrogen electrode (NHE).[36] Hence, on the basis of the observed values of V_{oc}, the platinized, methyl-terminated n-Si MW array electrodes did not generate sufficient photovoltage under 1 Sun of normal-incidence simulated AM1.5G solar illumination to simultaneously drive half-reaction 1 in conjunction with the reduction of protons to molecular hydrogen, half-reaction 2, each at standard state:

$$3I^- \rightleftharpoons I_3^- + 2e^- \quad (1)$$

$$2H^+ + 2e^- \rightleftharpoons H_2 \quad (2)$$

However, the V_{oc} values do allow for unassisted splitting of 7.6 M HI(aq), whose nonstandard-state concentration results in $E(I_3^-/I^-) \approx +0.25$ V.[37]

The combination of enhanced stability, catalysis, and large V_{oc} values is a key step toward use of MW arrays for integrated reversible storage of solar energy as H_2 using a variety of electron sources, such as other hydrohalic acids (e.g., HBr(aq)) or H_2O. The benefits of using hydrohalic acid fuel precursors are (i) some are abundant; (ii) the thermodynamics required for these reactions can be supplied by a single light-absorber material used in efficient and commercial photovoltaics; and (iii) the electron-transfer chemistry between most materials and halides is extremely rapid, resulting in little energy loss during repeated oxidations and reductions in a redox flow battery. These facts have led photoelectrochemical redox flow batteries to be an active area of research.[68−73] Toward this, inexpensive carbon-based materials could be deposited on Si MW arrays as electrodeposited organic polymers or high-surface-area graphitic materials, therefore enabling small overpotentials for the hydrohalic redox reactions and enabling a better match between the available current from unconcentrated sunlight and the load from the electrochemical reactions, catalysts, and electrolyte.[32]

■ ASSOCIATED CONTENT

Supporting Information

The Supporting Information is available free of charge on the ACS Publications website at DOI: 10.1021/acsenergylett.9b01529.

> Additional experimental details, mathematical analysis of Si microwire array stability, single Si microwire dopant density as a function of PH_3 flow rate, performance of a Si microwire array in nonaqueous electrolyte, spectral response of a Si microwire array in nonaqueous electrolyte, stability of a methylated Si microwire array in aqueous electrolyte, and scanning electron micrograph images of single Si microwires with electrochemically deposited Pt (PDF)

■ AUTHOR INFORMATION

Corresponding Author

*E-mail: nslewis@caltech.edu. Fax: +1 626 395-8867. Tel: +1 626 395-6335.

ORCID

Shane Ardo: 0000-0001-7162-6826
Ronald L. Grimm: 0000-0003-0407-937X
Harry A. Atwater: 0000-0001-9435-0201
Nathan S. Lewis: 0000-0001-5245-0538

Notes

The authors declare no competing financial interest.

■ ACKNOWLEDGMENTS

This work was supported by the National Science Foundation (NSF) Center for Chemical Innovation (CCI) Powering the Planet grants (Grants CHE-0802907, CHE-0947829, and NSF-ACCF) and made use of the Molecular Materials Resource Center of the Beckman Institute at Caltech and the Kavli Nanoscience Institute at Caltech. S.A. acknowledges support from a U.S. Department of Energy, Office of Energy Efficiency and Renewable Energy (EERE) Postdoctoral Research Award under the EERE Fuel Cell Technologies Program.

■ REFERENCES

(1) Jean, J.; Brown, P. R.; Jaffe, R. L.; Buonassisi, T.; Bulović, V. Pathways for Solar Photovoltaics. *Energy Environ. Sci.* **2015**, *8*, 1200−1219.

(2) U.S. Energy Information Administration. *Levelized Cost and Levelized Avoided Cost of New Generation Resources in the Annual Energy Outlook*; 2019.

(3) National Research Council. *The National Academies Summit on America's Energy Future*; Summary of a Meeting; 2008.

(4) Hou, Q.; Zhang, N.; Du, E.; Miao, M.; Peng, F.; Kang, C. Probabilistic Duck Curve in High PV Penetration Power System: Concept, Modeling, and Empirical Analysis in China. *Appl. Energy* **2019**, *242*, 205−215.

(5) Hou, Y.; Abrams, B. L.; Vesborg, P. C. K.; Björketun, M. E.; Herbst, K.; Bech, L.; Setti, A. M.; Damsgaard, C. D.; Pedersen, T.; Hansen, O.; et al. Bioinspired Molecular Co-Catalysts Bonded to a Silicon Photocathode for Solar Hydrogen Evolution. *Nat. Mater.* **2011**, *10*, 434−438.

(6) Warren, E. L.; Atwater, H. A.; Lewis, N. S. Silicon Microwire Arrays for Solar Energy-Conversion Applications. *J. Phys. Chem. C* **2014**, *118*, 747−759.

(7) Lewis, N. S. Developing a Scalable Artificial Photosynthesis Technology through Nanomaterials by Design. *Nat. Nanotechnol.* **2016**, *11*, 1010−1019.

(8) Chen, C.-J.; Yang, K.-C.; Liu, C.-W.; Lu, Y.-R.; Dong, C.-L.; Wei, D.-H.; Hu, S.-F.; Liu, R.-S. Silicon Microwire Arrays Decorated with Amorphous Heterometal-Doped Molybdenum Sulfide for Water Photoelectrolysis. *Nano Energy* **2017**, *32*, 422−432.

(9) Bazri, B.; Lin, Y.-C.; Lu, T.-H.; Chen, C.-J.; Kowsari, E.; Hu, S.-F.; Liu, R.-S. A Heteroelectrode Structure for Solar Water Splitting: Integrated Cobalt Ditelluride across a TiO_2-Passivated Silicon Microwire Array. *Catal. Sci. Technol.* **2017**, *7*, 1488−1496.

(10) Vijselaar, W.; Westerik, P.; Veerbeek, J.; Tiggelaar, R. M.; Berenschot, E.; Tas, N. R.; Gardeniers, H.; Huskens, J. Spatial Decoupling of Light Absorption and Catalytic Activity of Ni−Mo-Loaded High-Aspect-Ratio Silicon Microwire Photocathodes. *Nature Energy* **2018**, *3*, 185−192.

(11) Tung, C.-W.; Chuang, Y.; Chen, H.-C.; Chan, T.-S.; Li, J.-Y.; Chen, H. M. Tunable Electrodeposition of Ni Electrocatalysts onto Si Microwires Array for Photoelectrochemical Water Oxidation. *Particle & Particle Systems Characterization* **2018**, *35*, 1700321.

(12) Vijselaar, W.; Tiggelaar, R. M.; Gardeniers, H.; Huskens, J. Efficient and Stable Silicon Microwire Photocathodes with a Nickel Silicide Interlayer for Operation in Strongly Alkaline Solutions. *ACS Energy Letters* **2018**, *3*, 1086−1092.

(13) Milbrat, A.; Vijselaar, W.; Guo, Y.; Mei, B.; Huskens, J.; Mul, G. Integration of Molybdenum-Doped, Hydrogen-Annealed $BiVO_4$ with Silicon Microwires for Photoelectrochemical Applications. *ACS Sustainable Chem. Eng.* **2019**, *7*, 5034−5044.

(14) Zhou, Z.; Wu, S.; Li, L.; Li, L.; Li, X. Regulating the Silicon/Hematite Microwire Photoanode by the Conformal Al_2O_3 Intermediate Layer for Water Splitting. *ACS Appl. Mater. Interfaces* **2019**, *11*, 5978−5988.

(15) Goodey, A. P.; Eichfeld, S. M.; Lew, K.-K.; Redwing, J. M.; Mallouk, T. E. Silicon Nanowire Array Photoelectrochemical Cells. *J. Am. Chem. Soc.* **2007**, *129*, 12344−12345.

(16) Hwang, Y. J.; Boukai, A.; Yang, P. High Density n-Si/n-TiO_2 Core/Shell Nanowire Arrays with Enhanced Photoactivity. *Nano Lett.* **2009**, *9*, 410−415.

(17) Peng, K.-Q.; Wang, X.; Wu, X.-L.; Lee, S.-T. Platinum Nanoparticle Decorated Silicon Nanowires for Efficient Solar Energy Conversion. *Nano Lett.* **2009**, *9*, 3704−3709.

(18) Mayer, M. T.; Du, C.; Wang, D. Hematite/Si Nanowire Dual-Absorber System for Photoelectrochemical Water Splitting at Low Applied Potentials. *J. Am. Chem. Soc.* **2012**, *134*, 12406−12409.

(19) Oh, I.; Kye, J.; Hwang, S. Enhanced Photoelectrochemical Hydrogen Production from Silicon Nanowire Array Photocathode. *Nano Lett.* **2012**, *12*, 298−302.

(20) Foley, J. M.; Price, M. J.; Feldblyum, J. I.; Maldonado, S. Analysis of the Operation of Thin Nanowire Photoelectrodes for Solar Energy Conversion. *Energy Environ. Sci.* **2012**, *5*, 5203−5220.

(21) Liu, C.; Tang, J.; Chen, H. M.; Liu, B.; Yang, P. A Fully Integrated Nanosystem of Semiconductor Nanowires for Direct Solar Water Splitting. *Nano Lett.* **2013**, *13*, 2989−2992.

(22) Li, X.; Xiao, Y.; Zhou, K.; Wang, J.; Schweizer, S. L.; Sprafke, A.; Lee, J.-H.; Wehrspohn, R. B. Photoelectrochemical Hydrogen Evolution of Tapered Silicon Nanowires. *Phys. Chem. Chem. Phys.* **2015**, *17*, 800−804.

(23) Zhang, F.-Q.; Hu, Y.; Meng, X.-M.; Peng, K.-Q. Fabrication and Photoelectrochemical Properties of Silicon/Nickel Oxide Core/Shell Nanowire Arrays. *RSC Adv.* **2015**, *5*, 88209−88213.

(24) Kayes, B. M.; Atwater, H. A.; Lewis, N. S. Comparison of the Device Physics Principles of Planar and Radial p-n Junction Nanorod Solar Cells. *J. Appl. Phys.* **2005**, *97*, 114302.

(25) Spurgeon, J. M.; Walter, M. G.; Zhou, J.; Kohl, P. A.; Lewis, N. S. Electrical Conductivity, Ionic Conductivity, Optical Absorption, and Gas Separation Properties of Ionically Conductive Polymer Membranes Embedded with Si Microwire Arrays. *Energy Environ. Sci.* **2011**, *4*, 1772−1780.

(26) De Luna, P.; Hahn, C.; Higgins, D.; Jaffer, S. A.; Jaramillo, T. F.; Sargent, E. H. What Would It Take for Renewably Powered Electrosynthesis to Displace Petrochemical Processes? *Science* **2019**, *364*, No. eaav3506.

(27) Bents, D. J.; Scullin, V. J.; Chang, B.-J.; Johnson, D. W.; Garcia, C. P. *Hydrogen-Oxygen PEM Regenerative Fuel Cell Energy Storage System*; NASA Report, 2005; NASA/TM-2005-213381.

(28) Pellow, M. A.; Emmott, C. J. M.; Barnhart, C. J.; Benson, S. M. Hydrogen or Batteries for Grid Storage? A Net Energy Analysis. *Energy Environ. Sci.* **2015**, *8*, 1938−1952.

(29) Green, M. A.; Hishikawa, Y.; Dunlop, E. D.; Levi, D. H.; Hohl-Ebinger, J.; Ho-Baillie, A. W. Y. Solar Cell Efficiency Tables (Version 52). *Prog. Photovoltaics* **2018**, *26*, 427−436.

(30) Haynes, W. M. *CRC Handbook of Chemistry and Physics*, 92nd ed.; CRC Press: Boca Raton, FL, 2011.

(31) Bolts, J. M.; Bocarsly, A. B.; Palazzotto, M. C.; Walton, E. G.; Lewis, N. S.; Wrighton, M. S. Chemically Derivatized N-Type Silicon Photoelectrodes. Stabilization to Surface Corrosion in Aqueous Electrolyte Solutions and Mediation of Oxidation Reactions by Surface-Attached Electroactive Ferrocene Reagents. *J. Am. Chem. Soc.* **1979**, *101*, 1378−1385.

(32) Simon, R. A.; Wrighton, M. S. Stabilization of n-Type Silicon Photoanodes against Photoanodic Decomposition with Thin Films of Polyacetylene. *Appl. Phys. Lett.* **1984**, *44*, 930−932.

(33) Chen, Y. W.; Prange, J. D.; Dühnen, S.; Park, Y.; Gunji, M.; Chidsey, C. E. D.; McIntyre, P. C. Atomic Layer-Deposited Tunnel Oxide Stabilizes Silicon Photoanodes for Water Oxidation. *Nat. Mater.* **2011**, *10*, 539−544.

(34) Hu, S.; Shaner, M. R.; Beardslee, J. A.; Lichterman, M.; Brunschwig, B. S.; Lewis, N. S. Amorphous TiO_2 Coatings Stabilize Si, GaAs, and GaP Photoanodes for Efficient Water Oxidation. *Science* **2014**, *344*, 1005−1009.

(35) Braff, W. A.; Bazant, M. Z.; Buie, C. R. Membrane-Less Hydrogen Bromine Flow Battery. *Nat. Commun.* **2013**, *4*, 2346.

(36) Pourbaix, M. *Atlas of Electrochemical Equilibria in Aqueous Solutions*; Pergamon Press Ltd.: Houston, TX, 1966.

(37) Takabayashi, S. *Photoelectrochemical Solar Energy Conversion with Metal Nano-Dotted and Surface-Alkylated n-Type Silicon (n-Si) Electrodes*. Ph.D. Thesis, Osaka University, 2005.

(38) Boettcher, S. W.; Warren, E. L.; Putnam, M. C.; Santori, E. A.; Turner-Evans, D.; Kelzenberg, M. D.; Walter, M. G.; McKone, J. R.; Brunschwig, B. S.; Atwater, H. A.; et al. Photoelectrochemical Hydrogen Evolution Using Si Microwire Arrays. *J. Am. Chem. Soc.* **2011**, *133*, 1216−1219.

(39) Warren, E. L.; Boettcher, S. W.; Walter, M. G.; Atwater, H. A.; Lewis, N. S. pH-Independent, 520 mV Open-Circuit Voltages of Si/Methyl Viologen$^{2+/+}$ Contacts Through Use of Radial n$^+$p-Si Junction Microwire Array Photoelectrodes. *J. Phys. Chem. C* **2011**, *115*, 594−598.

(40) Kelzenberg, M. D.; Turner-Evans, D. B.; Putnam, M. C.; Boettcher, S. W.; Briggs, R. M.; Baek, J. Y.; Lewis, N. S.; Atwater, H. A. High-Performance Si Microwire Photovoltaics. *Energy Environ. Sci.* **2011**, *4*, 866−871.

(41) Ardo, S.; Park, S. H.; Warren, E. L.; Lewis, N. S. Unassisted Solar-Driven Photoelectrosynthetic HI Splitting Using Membrane-Embedded Si Microwire Arrays. *Energy Environ. Sci.* **2015**, *8*, 1484−1492.

(42) Bansal, A.; Lewis, N. S. Stabilization of Si Photoanodes in Aqueous Electrolytes through Surface Alkylation. *J. Phys. Chem. B* **1998**, *102*, 4058−4060.

(43) Grimm, R. L.; Bierman, M. J.; O'Leary, L. E.; Strandwitz, N. C.; Brunschwig, B. S.; Lewis, N. S. Comparison of the Photoelectrochemical Behavior of H-Terminated and Methyl-Terminated Si(111) Surfaces in Contact with a Series of One-Electron, Outer-Sphere Redox Couples in CH_3CN. *J. Phys. Chem. C* **2012**, *116*, 23569−23576.

(44) Maiolo, J. R.; Kayes, B. M.; Filler, M. A.; Putnam, M. C.; Kelzenberg, M. D.; Atwater, H. A.; Lewis, N. S. High Aspect Ratio Silicon Wire Array Photoelectrochemical Cells. *J. Am. Chem. Soc.* **2007**, *129*, 12346−12347.

(45) Boettcher, S. W.; Spurgeon, J. M.; Putnam, M. C.; Warren, E. L.; Turner-Evans, D. B.; Kelzenberg, M. D.; Maiolo, J. R.; Atwater, H. A.; Lewis, N. S. Energy-Conversion Properties of Vapor-Liquid-Solid-

Grown Silicon Wire-Array Photocathodes. *Science* **2010**, *327*, 185−187.

(46) Bansal, A.; Li, X.; Lauermann, I.; Lewis, N. S.; Yi, S. I.; Weinberg, W. H. Alkylation of Si Surfaces Using a Two-Step Halogenation/Grignard Route. *J. Am. Chem. Soc.* **1996**, *118*, 7225−7226.

(47) Yahyaie, I.; Ardo, S.; Oliver, D. R.; Thomson, D. J.; Freund, M. S.; Lewis, N. S. Comparison between the Electrical Junction Properties of H-Terminated and Methyl-Terminated Individual Si Microwire/Polymer Assemblies for Photoelectrochemical Fuel Production. *Energy Environ. Sci.* **2012**, *5*, 9789.

(48) Bruce, J. P.; Asgari, S.; Ardo, S.; Lewis, N. S.; Oliver, D. R.; Freund, M. S. Measurement of the Electrical Resistance of n-Type Si Microwire/p-Type Conducting Polymer Junctions for Use in Artificial Photosynthesis. *J. Phys. Chem. C* **2014**, *118*, 27742−27748.

(49) Koren, E.; Rosenwaks, Y.; Allen, J. E.; Hemesath, E. R.; Lauhon, L. J. Nonuniform Doping Distribution along Silicon Nanowires Measured by Kelvin Probe Force Microscopy and Scanning Photocurrent Microscopy. *Appl. Phys. Lett.* **2009**, *95*, 092105.

(50) Koren, E.; Berkovitch, N.; Rosenwaks, Y. Measurement of Active Dopant Distribution and Diffusion in Individual Silicon Nanowires. *Nano Lett.* **2010**, *10*, 1163−1167.

(51) Kelzenberg, M. D.; Boettcher, S. W.; Petykiewicz, J. A.; Turner-Evans, D. B.; Putnam, M. C.; Warren, E. L.; Spurgeon, J. M.; Briggs, R. M.; Lewis, N. S.; Atwater, H. A. Enhanced Absorption and Carrier Collection in Si Wire Arrays for Photovoltaic Applications. *Nat. Mater.* **2010**, *9*, 239−244.

(52) Santori, E. A.; Maiolo, J. R., III; Bierman, M. J.; Strandwitz, N. C.; Kelzenberg, M. D.; Brunschwig, B. S.; Atwater, H. A.; Lewis, N. S. Photoanodic Behavior of Vapor-Liquid-Solid−Grown, Lightly Doped, Crystalline Si Microwire Arrays. *Energy Environ. Sci.* **2012**, *5*, 6867−6871.

(53) Yalamanchili, S.; Kempler, P. A.; Papadantonakis, K. M.; Atwater, H. A.; Lewis, N. S. Integration of Electrocatalysts with Silicon Microcone Arrays for Minimization of Optical and Overpotential Losses during Sunlight-Driven Hydrogen Evolution. *Sustainable Energy Fuels* **2019**; DOI: 10.1039/C9SE00294D.

(54) Lewis, N. S.; Bocarsly, A. B.; Wrighton, M. S. Heterogeneous Electron Transfer at Designed Semiconductor/Liquid Interfaces. Rate of Reduction of Surface-Confined Ferricenium Centers by Solution Reagents. *J. Phys. Chem.* **1980**, *84*, 2033−2043.

(55) Bocarsly, A. B.; Walton, E. G.; Wrighton, M. S. Use of Chemically Derivatized n-Type Silicon Photoelectrodes in Aqueous Media. Photooxidation of Iodide, Hexacyanoiron(II), and Hexaammineruthenium(II) at Ferrocene-Derivatized Photoanodes. *J. Am. Chem. Soc.* **1980**, *102*, 3390−3398.

(56) Maldonado, S.; Plass, K. E.; Knapp, D.; Lewis, N. S. Electrical Properties of Junctions between Hg and Si(111) Surfaces Functionalized with Short-Chain Alkyls. *J. Phys. Chem. C* **2007**, *111*, 17690−17699.

(57) Johansson, E.; Boettcher, S. W.; O'Leary, L. E.; Poletayev, A. D.; Maldonado, S.; Brunschwig, B. S.; Lewis, N. S. Control of the pH-Dependence of the Band Edges of Si(111) Surfaces Using Mixed Methyl/Allyl Monolayers. *J. Phys. Chem. C* **2011**, *115*, 8594−8601.

(58) Sze, S. M.; Ng, K. K. *Physics of Semiconductor Devices*, 3rd ed.; John Wiley & Sons, Inc.: Hoboken, NJ, 2007.

(59) Nakato, K.; Takabayashi, S.; Imanishi, A.; Murakoshi, K.; Nakato, Y. Stabilization of n-Si Electrodes by Surface Alkylation and Metal Nano-Dot Coating for Use in Efficient Photoelectrochemical Solar Cells. *Sol. Energy Mater. Sol. Cells* **2004**, *83*, 323−330.

(60) Bruce, J. P. *Surface Functionalization of Silicon Microwires for Use in Artificial Photosynthetic Devices*. M.S. Thesis, University of Manitoba, 2014.

(61) Wong, K. T.; Lewis, N. S. What a Difference a Bond Makes: The Structural, Chemical, and Physical Properties of Methyl-Terminated Si(111) Surfaces. *Acc. Chem. Res.* **2014**, *47*, 3037−3044.

(62) Deutsch, T.; Turner, J.; Leisch, J.; Wang, H.; Welch, A.; Lindeman, A.; O'Neill, K.; Pinkard, A.; Dameron, A.; Heske, C.; et al. Stable Photoelectrode Surfaces and Methods. U.S. Patent 20140332374 A1, November 13,2014.

(63) Nielander, A. C.; Bierman, M. J.; Petrone, N.; Strandwitz, N. C.; Ardo, S.; Yang, F.; Hone, J.; Lewis, N. S. Photoelectrochemical Behavior of n-Type Si(111) Electrodes Coated with a Single Layer of Graphene. *J. Am. Chem. Soc.* **2013**, *135*, 17246−17249.

(64) Sikes, H. D.; Smalley, J. F.; Dudek, S. P.; Cook, A. R.; Newton, M. D.; Chidsey, C. E.; Feldberg, S. W. Rapid Electron Tunneling through Oligophenylenevinylene Bridges. *Science* **2001**, *291*, 1519−1523.

(65) Bookbinder, D. C.; Bruce, J. A.; Dominey, R. N.; Lewis, N. S.; Wrighton, M. S. Synthesis and Characterization of a Photosensitive Interface for Hydrogen Generation: Chemically Modified p-Type Semiconducting Silicon Photocathodes. *Proc. Natl. Acad. Sci. U. S. A.* **1980**, *77*, 6280−6284.

(66) Abruna, H. D.; Bard, A. J. Semiconductor Electrodes. 40. Photoassisted Hydrogen Evolution at Poly(Benzyl Viologen)-Coated p-Type Silicon Electrodes. *J. Am. Chem. Soc.* **1981**, *103*, 6898−6901.

(67) Trotochaud, L.; Mills, T. J.; Boettcher, S. W. An Optocatalytic Model for Semiconductor−Catalyst Water-Splitting Photoelectrodes Based on In Situ Optical Measurements on Operational Catalysts. *J. Phys. Chem. Lett.* **2013**, *4*, 931−935.

(68) Liu, P.; Cao, Y.; Li, G.-R.; Gao, X.-P.; Ai, X.-P.; Yang, H.-X. A Solar Rechargeable Flow Battery Based on Photoregeneration of Two Soluble Redox Couples. *ChemSusChem* **2013**, *6*, 802−806.

(69) Yu, M.; McCulloch, W. D.; Beauchamp, D. R.; Huang, Z.; Ren, X.; Wu, Y. Aqueous Lithium−Iodine Solar Flow Battery for the Simultaneous Conversion and Storage of Solar Energy. *J. Am. Chem. Soc.* **2015**, *137*, 8332−8335.

(70) McCulloch, W. D.; Yu, M.; Wu, Y. pH-Tuning a Solar Redox Flow Battery for Integrated Energy Conversion and Storage. *ACS Energy Letters* **2016**, *1*, 578−582.

(71) McKone, J. R.; DiSalvo, F. J.; Abruña, H. D. Solar Energy Conversion, Storage, and Release Using an Integrated Solar-Driven Redox Flow Battery. *J. Mater. Chem. A* **2017**, *5*, 5362−5372.

(72) Li, W.; Fu, H.-C.; Zhao, Y.; He, J.-H.; Jin, S. 14.1% Efficient Monolithically Integrated Solar Flow Battery. *Chem.* **2018**, *4*, 2644−2657.

(73) Liao, S.; Zong, X.; Seger, B.; Pedersen, T.; Yao, T.; Ding, C.; Shi, J.; Chen, J.; Li, C. Integrating a Dual-Silicon Photoelectrochemical Cell into a Redox Flow Battery for Unassisted Photocharging. *Nat. Commun.* **2016**, *7*, 11474.